CIPM MRA
Comparison reports

BIPM.RI(I)-K6 (NPL 2025)

Measurement of absorbed dose to water for high-energy photon beams

KEY COMPARISON

Any further distribution of this Report must be cited as:
C. Kessler *et al* 2026 *CIPM MRA Comparison reports* **06009**

https://doi.org/10.59161/TJVV2367

Comparison BIPM.RI(I)-K6 of the standards for absorbed dose to water of the NPL, United Kingdom and the BIPM in accelerator photon beams

C. Kessler[1], P. Roger[1], T. Sander[2], G. Bass[2], F. Blake Parsons[2]

[1] Bureau International des Poids et Mesures, F-92310 Sèvres Cedex
[2] National Physical Laboratory, Teddington, Middlesex, United Kingdom

Abstract

A key comparison has been made between the absorbed dose to water standards of the National Physical Laboratory (NPL), United Kingdom, and the Bureau International des Poids et Mesures (BIPM) in accelerator photon beams. The results show the standards to be in agreement within the standard uncertainty of the comparison of 7.7 parts in 10^3. The results are analysed and presented in terms of degrees of equivalence, suitable for entry in the BIPM key comparison database.

1. Introduction

A new comparison has been made between the absorbed dose to water standards of the National Physical Laboratory (NPL), United Kingdom, and the Bureau International des Poids et Mesures (BIPM) in the accelerator photon beam range from 6 MV to 18 MV. The results are published in the BIPM key comparison database (KCDB 2026) under the reference BIPM.RI(I)-K6. The BIPM measurements took place using the accelerator facility at the DOSEO platform in Saclay (France) in September 2025. The comparison was undertaken in three radiation beams using two transfer ionization chambers belonging to the NPL. The results of the comparison are given in terms of the mean ratio of the calibration coefficients of the two transfer chambers determined at the two laboratories for each radiation quality. The final results were supplied by the NPL in December 2025.

2. Irradiation facilities

2.1 The BIPM irradiation facility and reference beam qualities

The BIPM measurements were carried out at the DOSEO platform in Saclay (France), which houses an Elekta Versa HD clinical linear accelerator, which has been characterized for use as a BIPM reference facility. This accelerator provides three high-energy photon beams at 6 MV, 10 MV and 18 MV. The radiation qualities are characterized in terms of the tissue-phantom ratio $TPR_{20,10}$, the measured values given in Table 1. Details of the BIPM measurement conditions are described by Kessler and Burns (2024).

All measurements were made with the gantry fixed for horizontal irradiation, with a source-detector distance of 1 m and at the reference depth of 10 g cm^{-2}.

The irradiation area at the DOSEO platform is temperature controlled in the range from 20 °C to 22 °C. Calibrated thermistors measure the temperature of the ambient air and the water. Air pressure is measured by means of a calibrated barometer positioned at the height of the beam axis. The relative humidity is controlled within the range from 40 % to 50 %. For the comparison measurements, the beam output was monitored during irradiation using a commercial parallel-plate transmission chamber fixed to a shadow tray.

2.2 The NPL irradiation facility and reference beam qualities

The NPL measurements were carried out at the NPL using an Elekta Versa HD clinical linear accelerator. It provides seven high-energy photon qualities, from which the 6 MV, 10 MV and 15 MV beams were selected to calibrate the transfer chambers for the present comparison. The radiation beams, characterized in terms of the tissue-phantom ratio $TPR_{20,10}$, are included in Table 1.

Measurements were made with the gantry fixed for horizontal irradiation, with a source-detector distance of 1 m and at the reference depth of 5 g cm^{-2} for the 6 MV and 10 MV photon beams, and at the reference depth of 7 g cm^{-2} for the 15 MV photon beam. The internal radiation monitor of the linear accelerator was used for the beam monitoring.

Table 1. Beam qualities

Radiation quality	6 MV	10 MV	15 MV	18 MV
BIPM $TPR_{20,10}$	0.686	0.733	---	0.774
NPL $TPR_{20,10}$	0.682	0.733	0.758	---

3. Details of the standards

3.1 BIPM primary standard

The BIPM primary standard is based on a graphite calorimeter described by Picard *et al.* (2009). The calorimeter consists of a graphite core placed in a cylindrical graphite jacket; the main characteristics are listed in Table 2.

Table 2. Characteristics of the BIPM standard

BIPM standard		Nominal values
Calorimeter core	Diameter / mm	45.0
	Thickness / mm	6.7
Calorimeter jacket	Diameter / mm	60.0
	Thickness / mm	32.0
Standard chamber	Diameter / mm	45.0
	Thickness / mm	11.0
Air cavity	Volume / cm^3	6.8
Wall	Thickness / mm	2.85
Wall material	Graphite of density / g cm^{-3}	1.85
Polarizing voltage	Applied to outer electrode / V	+80

The core is equipped with three thermistor pairs connected to three independent d.c. bridges. The core and the jacket are placed in an evacuated cubic polymethyl methacrylate (PMMA) vacuum phantom with side length 300 mm. A graphite build-up plate is used to position the calorimeter centre at the reference depth of 10 g cm^{-2}. Two nominally identical parallel-plate ionization chamber standards with graphite walls and collectors, similar in design to the existing BIPM ^{60}Co standards for air kerma and absorbed dose to water, were constructed to serve in the determination of the absorbed dose to water from the measured absorbed dose to the graphite core. The first chamber is housed in a graphite jacket, nominally identical to the calorimeter jacket, and is positioned in the same PMMA vacuum phantom but at ambient air pressure, replacing the calorimeter core and its jacket. The second chamber is housed in a waterproof PMMA sleeve and mounted at a depth of 10 g cm^{-2} in a PMMA water phantom with the same outer dimensions and PMMA window thickness (4 mm) as the vacuum phantom.

3.2 NPL primary standard

The NPL primary standard is based on a graphite calorimeter, described by Sander *et al.* (2017) and Kessler *et al.* (2019a). The calorimeter consists of a cylindrical graphite core, surrounded by an inner and outer graphite jacket, and a graphite body (mantle). Heating and sensing thermistors are embedded in the graphite parts. All four graphite parts are mounted inside a polyether ether ketone (PEEK) vacuum enclosure and separated from each other by sub-millimetre vacuum gaps. The rear and side walls of the PEEK enclosure are surrounded by a cylindrical outer graphite phantom. Graphite build-up plates are positioned in front of the PEEK housing to achieve water-equivalent reference depths of either 5 g cm^{-2} at the centre of the core for photon beams up to and including 10 MV, or 7 g cm^{-2} for photon beams above 10 MV. The calorimeter is operated in quasi-adiabatic mode, and the sensitivity of the calorimeter to ionizing radiation energy absorbed in the graphite core is calculated from voltage and resistance measurements traceable to standards of the NPL. The absorbed dose to water is determined from calorimetric measurements of the absorbed dose to graphite (see section 4.3).

The main characteristics of the NPL calorimeter are shown in Table 3.

Table 3. Characteristics of the NPL graphite calorimeter

Component	Characteristic	Value
Core	Diameter / mm	19.984
	Thickness / mm	5.005
	Effective mass / g	2.9572
	Graphite density / g cm^{-3}	1.878
Gap widths	Gap between core and inner front jacket / mm	0.768
	Gap between inner and outer front jacket / mm	0.769
	Gap between outer front jacket and outer front mantle / mm	0.822
Water-equivalent depth	Mid-plane of core to front of phantom (excl. build-up) / g cm^{-2}	1.5558
Cylindrical outer graphite phantom	Diameter / cm	32
	Height (excl. build-up) / cm	8.26
Cylindrical build-up plate	Diameter / cm	23
	Height (for measurements at 5 g cm^{-2}) / cm	2.08
	Height (for measurements at 7 g cm^{-2}) / cm	3.29
	Graphite density (mean) / g cm^{-3}	1.841

Note: All the calorimeter components were constructed from a single block of graphite. The build-up plates, however, were constructed from a different type of graphite with the density stated in the table.

4. Determination of the absorbed dose to water

4.1 Absorbed dose to water at the BIPM: formalism and method

The BIPM determination of absorbed dose to water is based on calorimetric and ionometric measurements combined with Monte Carlo calculations. The method is described in the previous BIPM.RI(I)-K6 comparison report between the BIPM and the NPL (Picard *et al.* 2015) and details of the standard are given in Kessler and Burns (2024). The absorbed dose to water at the reference depth, $D_{\mathrm{w,BIPM}}$, is evaluated as

$$D_{\mathrm{w,BIPM}} = D_{\mathrm{c}} \frac{Q_{\mathrm{w,st}}}{Q_{\mathrm{c,st}}} \left(\frac{D_{\mathrm{w}}}{D_{\mathrm{c}}}\right)^{\mathrm{MC}} \left(\frac{D_{\mathrm{cav,c}}}{D_{\mathrm{cav,w}}}\right)^{\mathrm{MC}} k_{\mathrm{rn,st}} \tag{1}$$

where:

D_{c}	measured absorbed dose to the graphite core,
$Q_{\mathrm{c,st}}$	ionization charge measured by the standard chamber positioned in the graphite jacket, replacing the core,
$Q_{\mathrm{w,st}}$	ionization charge measured by the standard chamber positioned in water,
$(D_{\mathrm{w}}/D_{\mathrm{c}})^{\mathrm{MC}}$	calculated ratio of absorbed dose to water and to the graphite core using Monte Carlo simulations,
$\left(D_{\mathrm{cav,c}}/D_{\mathrm{cav,w}}\right)^{\mathrm{MC}}$	calculated ratio of cavity doses in graphite and in water using Monte Carlo simulations, and
$k_{\mathrm{rn,st}}$	measured correction for radial non-uniformity for the standard chamber in water.

The ionization charges $Q_{\mathrm{w,st}}$ and $Q_{\mathrm{c,st}}$ are normalized to 293.15 K and 101.325 kPa and corrected for ion recombination. In practice, two nominally identical standard chambers are used; the air cavity volume for each is known and a correction $k_{\mathrm{vol,st}}$ is made for the small difference in volume with a relative standard uncertainty of 3 parts in 10^4.

Equation 1 can also be expressed as

$$\begin{aligned} D_{\mathrm{w,BIPM}} &= Q_{\mathrm{w,st}} \frac{D_{\mathrm{c}}}{Q_{\mathrm{c,st}}} C_{\mathrm{w,c}} k_{\mathrm{rn,st}} \\ &= Q_{\mathrm{w,st}} N_{D,\mathrm{c,st}} C_{\mathrm{w,c}} k_{\mathrm{rn,st}} \end{aligned} \tag{2}$$

where:

$C_{\mathrm{w,c}}$	represents the total Monte Carlo conversion factor, and
$N_{D,\mathrm{c,st}}$	is the measured calibration coefficient for the standard chamber in graphite.

The conversion factor $C_{\mathrm{w,c}}$ and the calibration coefficients $N_{D,\mathrm{c,st}}$ for the standard chamber in graphite for given $\mathrm{TPR}_{20,10}$ values are taken to be those derived from quadratic fits, as explained in Kessler *et al.* (2019b). Figure 1 shows the conversion factors plotted as a function of the calculated $\mathrm{TPR}_{20,10}$, calculated for the beams of seven National Metrology Institutes (NMIs) that participated in the BIPM.RI(I)-K6 key comparison.

Figure 2 shows the normalized $N_{D,\mathrm{c,st}}$ determinations and a quadratic fit to the data; the plot shows the coefficients determined at all the NMIs that participated in the BIPM.RI(I)-K6 key comparison and at the DOSEO facility in Saclay (France). These latter data are included in the fit.

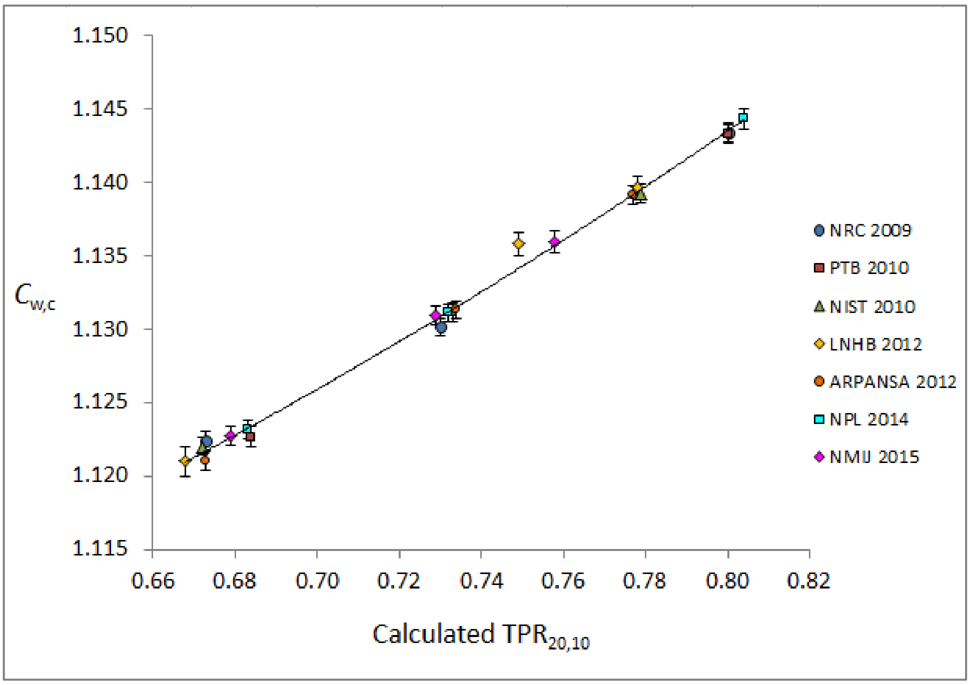

Figure 1. The dose conversion factor $C_{w,c}$ for the BIPM standard, calculated using the phase-space files supplied by participating NMIs. The line is a weighted quadratic fit to the data; the deviations about this line are consistent with the typical statistical standard uncertainty of 5 parts in 10^4.

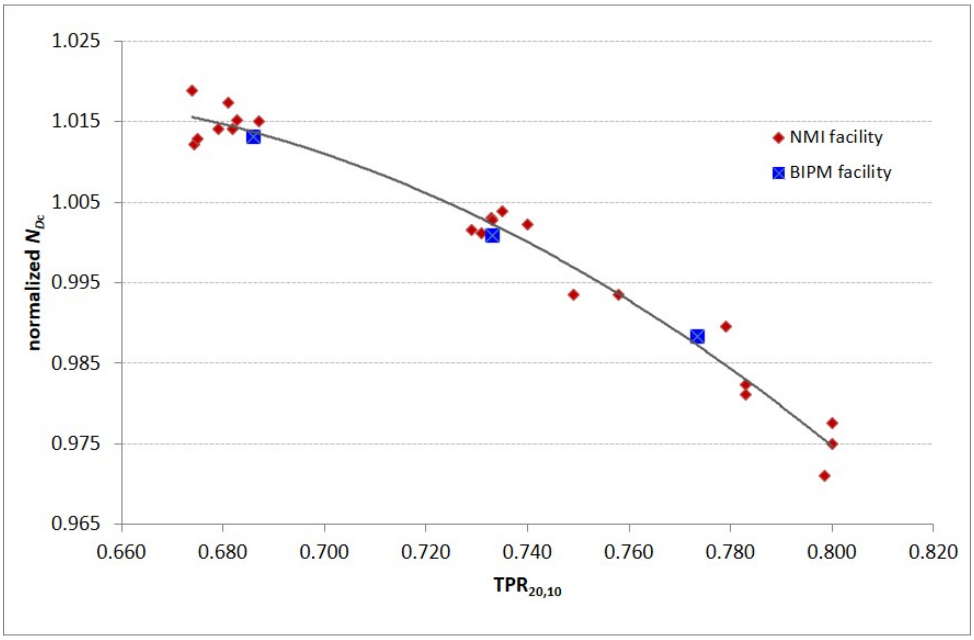

Figure 2. The calibration coefficients $N_{D,c,st}$ determined by the BIPM at various NMI facilities (red) and at the BIPM facility (blue), normalized to the mean, as a function of the measured $TPR_{20,10}$. The solid line is a quadratic fit to the combined data set.

4.2 Absorbed dose to water at the BIPM: practical determination

For the present comparison, instead of using the standard chamber in water, a NE 2571 chamber was used as the BIPM reference. Since 2017, this chamber has been calibrated periodically against the primary standard and has been fully characterized to be considered as a reference chamber. The relative standard uncertainty corresponding to the long-term stability of its calibration coefficient $N_{D,\mathrm{w,ref\ ch}}$ is 6 parts in 10^4, included in Table 11.

The absorbed dose to water was thus determined as

$$D_{\mathrm{w,BIPM}} = Q_{\mathrm{w,ref\ ch}} N_{D,\mathrm{w,ref\ ch}} k_{\mathrm{rn,ref\ ch}} k_{\mathrm{s,ref\ ch}} \tag{3}$$

where:

$Q_{\mathrm{w,ref\ ch}}$	ionization charge measured by the reference chamber positioned in water (normalized to the monitor chamber),
$N_{D,\mathrm{w,ref\ ch}}$	calibration coefficient of the reference chamber,
$k_{\mathrm{rn,ref\ ch}}$	radial non-uniformity correction factor for the reference chamber, and
$k_{\mathrm{s,ref\ ch}}$	ion recombination correction factor for the reference chamber.

The ionization charge $Q_{\mathrm{w,ref\ ch}}$ is normalized to 293.15 K and 101.325 kPa; no correction for humidity is applied.

The correction factor $k_{\mathrm{s,ref\ ch}}$ for losses due to ion recombination for the reference chamber was determined using the method of Niatel as described by Boutillon (1998) for continuous radiation and implemented for pulsed radiation by Picard *et al.* (2011). The ion recombination correction factor for pulsed radiation, k_{s}, can be expressed as:

$$k_{\mathrm{s}} = 1 + k_{\mathrm{init}} + k_{\mathrm{vol}} Q_{\mathrm{p}} \tag{4}$$

where Q_{p} is the charge per pulse expressed in pC, k_{init} is the initial recombination and diffusion and k_{vol} is the volume recombination coefficient. Table 4 gives the values for k_{init} and k_{vol} for the reference chamber, for the operating voltage of 250 V. For a typical charge per pulse of up to 10 pC, $k_{\mathrm{s,ref\ ch}}$ is of the order of 1 part in 10^2 and the standard uncertainty for $k_{\mathrm{s,ref\ ch}}$ is estimated to be 3 parts in 10^4, as shown in Table 11. The correction factors for the three radiation qualities are presented in Table 5.

Table 4. Ion recombination for the BIPM reference chamber NE 2571

Coefficient	Value
initial recombination and diffusion, k_{init}	12.9×10^{-4}
volume recombination coefficient, k_{vol} / pC^{-1}	7.1×10^{-4}

The factors that correct for the non-uniformity of the beams were calculated from the beam profiles in water measured by the BIPM. For thimble chamber types of similar dimensions to the NE 2571, the correction factors for the three different beams are presented in Table 5 with an estimated relative standard uncertainty for both of 3 parts in 10^4, as shown in Table 11. Note that these corrections will largely cancel when the reference chamber is used to calibrate a transfer chamber of similar dimensions.

Table 5. Correction factors for the BIPM reference chamber NE 2571

Radiation quality	6 MV	10 MV	18 MV
ion recombination $k_{\mathrm{s,ref\ ch}}$	1.0038	1.0064	1.0076
radial non-uniformity $k_{\mathrm{rn,ref\ ch}}$	1.0000	0.9980	1.0000

4.3 Absorbed dose to water at the NPL: determination of $N_{D,\mathrm{w,lab}}$

As explained in section 3.2, the absorbed dose to water at the NPL is determined from calorimetric measurements of the absorbed dose to graphite. The absorbed dose to graphite, $D_{\mathrm{g,ref}}$, at the reference point (equivalent to either 5 g cm^{-2} depth in water for photon beams up to and including 10 MV, or 7 g cm^{-2} depth in water for photon beams above 10 MV) in a homogeneous, cylindrical, pure graphite phantom (with the shape of the calorimeter components and their sizes scaled in terms of electron density) is given by

$$D_{\mathrm{g,ref}} = \left(E^{\mathrm{rad}}/m_{\mathrm{core,eff}}\right)k_{\mathrm{imp}}k_{\mathrm{gap}}k_{\mathrm{z,cal}}k_{\mathrm{d,cal}}k_{\mathrm{rn,cal}}k_{\mathrm{an,cal}} \quad (5)$$

where:

E^{rad} is the energy absorbed in the calorimeter core from ionizing radiation only (Seuntjens and Duane 2009),

$m_{\mathrm{core,\,eff}}$ is the effective mass of the graphite core including all non-graphite materials,

k_{imp} is the Monte Carlo (MC) calculated impurity correction factor, calculated as the dose ratio $D_{\mathrm{core,gaps}}$ / $D_{\mathrm{core,all}}$, where $D_{\mathrm{core,gaps}}$ is the dose to the core with all non-graphite materials in the calorimeter substituted with pure graphite (no impurities) with mass density of the core graphite and scaled in terms of electron density, and $D_{\mathrm{core,all}}$ is the dose to the core in the real calorimeter,

k_{gap} is the MC calculated compensated vacuum gap correction factor, calculated as the dose ratio $D_{\mathrm{core,nogaps}}$ / $D_{\mathrm{core,gaps}}$, where $D_{\mathrm{core,nogaps}}$ is the dose to the core with all vacuum gaps in the pure graphite calorimeter geometry substituted with pure graphite ensuring the mass-thickness (in terms of electron density) of material upstream of the graphite core remains unchanged, and $D_{\mathrm{core,\,gaps}}$ is defined as above,

$k_{\mathrm{z,cal}}$ is the inverse square correction factor for the difference in distance between the linear accelerator (linac) photon source to the reference plane and the linac photon source to the measurement plane (centre of calorimeter core),

$k_{\mathrm{d,cal}}$ is the correction factor for the difference in the desired reference depth in graphite and that achievable in the measurement setup,

$k_{\mathrm{rn,cal}}$ is the correction factor for the radial non-uniformity of the linac photon beam over the calorimeter core, and

$k_{\mathrm{an,cal}}$ is the correction factor for the axial non-uniformity of the linac photon beam over the calorimeter core. The decrease of absorbed dose with depth at the water-equivalent depth of 5 g cm^{-2} for photon beams up to and including 10 MV, and 7 g cm^{-2} for photon beams above 10 MV, is approximately linear and, as the calorimeter core extends only 5 mm along the beam axis, no correction is made for the non-uniformity of absorbed dose along the beam axis.

The previously applied thermistor lead resistance correction factor $k_{\mathrm{lead\ res,th}}$ in Sander *et al.* (2017) and Kessler *et al.* (2019) was removed from Equation (5) in this report and deemed to be more appropriate to be included in the uncertainty budget (see Table 13, item 'Electrical calibrations').

The NPL reference standards

The NPL uses a set of three reference standard ionization chambers, two manufactured by Nuclear Enterprises of type NE 2611A, serial numbers 202 and 204, and one manufactured by NPL of type NPL 2611, serial number 1010, to maintain and transfer absorbed dose to graphite (Pearce *et al.* 2011). The main characteristics of these reference standards are listed in Table 6. The same types of ionization chambers were used as transfer chambers for this comparison (see section 5).

Table 6. Characteristics of the NPL reference standard and transfer chambers

Dimensions		NE 2611A / NPL 2611
Chamber	Cavity diameter / mm	7.35
	Cavity length / mm	9.22
Electrode	Diameter / mm	1.76
	Length / mm	6.35
Cavity	Nominal volume / cm^3	0.325
Wall	Thickness / mm	0.5
	Material	Graphite
	Density / g cm^{-3}	1.80
Voltage applied to the outer electrode / V		-200

The reference standard chambers are set up in a cuboidal graphite phantom and calibrated against the calorimeter.

The dose to graphite at the reference point at the centre of the thimble chamber inside the graphite phantom, D_g, measured at 5.0426 g cm^{-2} or 6.9447 g cm^{-2} water-equivalent depth in terms of electron density for photon beams up to and including 10 MV, and above 10 MV, respectively, is given by

$$D_{\mathrm{g}} = D_{\mathrm{g,ref}}\, k_{\mathrm{geom}} \tag{6}$$

where:

$D_{\mathrm{g,ref}}$ is the absorbed dose to graphite at the reference point in the graphite core of the calorimeter (water-equivalent depth of 5 or 7 g cm^{-2}) and

k_{geom} is the MC calculated configuration correction factor for the combined effect of
(a) the difference between the geometries of the cylindrical calorimeter and the cuboidal graphite phantom, which is used to calibrate NPL's reference standard chambers, resulting in different scatter contributions at the reference point, and
(b) the difference in depth of the reference points for the calorimeter (5 or 7 g cm^{-2}) and the graphite phantom (5.0426 or 6.9447 g cm^{-2}).
k_{geom} corrects $D_{\mathrm{g,ref}}$ to the measurement point of the reference standard chamber in the graphite phantom, where the chamber is not at exactly 5 or 7 g cm^{-2} water-equivalent depth.

The reference standard calibration coefficient, $N_{D,\mathrm{g,NPLref\ cham}}$, in terms of absorbed dose to graphite per unit electric charge produced in the thimble chamber inside the graphite phantom is obtained from the relation

$$N_{D,\mathrm{g,\ NPL\ ref\ cham}} = D_{\mathrm{g}} / (Q_{\mathrm{g,\ NPL\ ref\ cham}}\, k_{\mathrm{elec}}\, k_{\mathrm{ion}}\, k_{\mathrm{z,cham}}\, k_{\mathrm{rn,cham}}\, k_{Tp}) \tag{7}$$

where:

D_{g} is the absorbed dose to graphite at the reference point in the graphite phantom (equivalent to 5.0426 or 6.9447 g cm^{-2} water-equivalent depth),

$Q_{\mathrm{g,\ NPL\ ref\ cham}}$ is the electric charge, measured at a relative humidity in the range 20 % to 70 %, with the reference standard chamber in the graphite phantom,

k_{elec} is the electrometer correction factor,

k_{ion} is the correction factor for ion recombination in the reference standard chamber,

$k_{\text{z, cham}}$ is the inverse square correction factor for the difference in distance between the linac photon source to the reference plane and the linac photon source to the measurement plane (centre of reference standard chamber),

$k_{\text{rn, cham}}$ is the correction factor for the radial non-uniformity of the linac photon beam over the reference standard chamber in the graphite phantom and

k_{Tp} is the factor to correct from ambient temperature T and pressure p to standard temperature and pressure.

Conversion to absorbed dose to water from absorbed dose to graphite

At the NPL, the reference standard chamber calibration coefficient, $N_{D\text{w,NPLref cham}}$, in terms of absorbed dose to water at the reference depth of 5 or 7 g cm^{-2} in water has been obtained from the reference standard chamber calibration coefficient, $N_{D\text{g,NPLref cham}}$, in terms of absorbed dose to graphite at the reference point (see Equation 7) by using the scaling dose ratio method and the formalism described by Nutbrown *et al.* (2002):

$$N_{D,\text{w, NPL ref cham}} = N_{D,\text{g, NPL ref cham}}\left(N_\text{w}/N_\text{g}\right) \tag{8}$$

where:

N_w / N_g is the conversion factor of the reference standard chamber calibration coefficient from graphite to water at the reference point.

N_w / N_g conversion factors for the NPL clinical linac MV photon beam qualities were taken from Pearce *et al.* (2010).

The uncertainty components for the determination of the absorbed-dose-to-water using the graphite calorimeter in combination with the reference standard chambers are shown in Table 13.

5. Comparison procedure

The comparison of the NPL and BIPM standards was carried out indirectly using the calibration coefficients $N_{D,\text{w,lab}}$ for two transfer chambers given by

$$N_{D,\text{w,lab}} = \dot{D}_{\text{w,lab}}/I_{\text{lab}} \tag{9}$$

where $\dot{D}_{\text{w, lab}}$ is the absorbed dose to water rate determined by a given laboratory, the NPL or the BIPM, and I_{lab} is the corresponding ionization current for a transfer chamber measured by each laboratory, using its own measurement system and corrected by the effects and influences described in this section.

The transfer chambers used for this comparison were the NPL owned ionization chambers NE 2611A, serial number 203 and NPL 2611, serial number 1007. Their main characteristics are the same as those for the reference standard chambers listed in Table 6.

The essential details for the determination of the calibration coefficients $N_{D,\text{w}}$ for the transfer chambers are described below.

Positioning

The transfer chambers were positioned by each laboratory inside the water-proof sleeve supplied by the NPL with the stem perpendicular to the beam direction and with the text on the stem facing the source.

Applied voltage and polarity

At the NPL and at the BIPM, a polarizing voltage of 200 V (negative polarity) was applied to the outer electrode (wall) of the transfer chambers. At the NPL, this was applied at least 10 minutes before any measurements were made. At the BIPM, the polarizing voltage was applied at least 30 minutes before any measurements were made. No corrections were applied by either laboratory for polarity.

Charge and current measurements

The charge was measured by the BIPM using a Keithley electrometer, model 6517, and a set of calibrated external capacitors. The capacitors are in a sealed box with a desiccant to minimize the moisture content. At the NPL, the ionization current was measured using a Keithley electrometer, model 6517A. The chambers were pre-irradiated for at least 10 minutes (≈ 20 Gy) by the BIPM and about 2 minutes by the NPL (≈ 10 Gy) before any measurements were made.

Ambient conditions

For the BIPM and NPL arrangements, the water temperature was measured for each current or charge measurement and it was stable to better than 0.1 °C at the BIPM and 0.2 °C at the NPL. The ionization current was normalized to 293.15 K and 101.325 kPa for both laboratories. Relative humidity was in the range from 40 % to 60 % at both facilities. No correction for humidity was applied to the ionization current measured by either laboratory.

Ion recombination

Ion recombination was measured by the BIPM for each chamber using the Niatel method as described previously using Equation 4. Table 7 gives the values for k_{init} and k_{vol}, for each chamber, for the operating voltage of 200 V. Ion recombination was also determined using the two-voltage method, as described in the TRS 398 protocol (IAEA 2000). The results obtained using both methods are presented in Table 8, showing a general agreement of 2 parts in 10^4. For the NPL, the correction for ion recombination was determined using the method described by Burns and Rosser (1990). This is also shown in Table 8.

Table 7. Ion recombination for the NPL transfer chambers determined at the BIPM

Coefficient	NE 2611A-203	NPL 2611-1007
initial recombination and diffusion, k_{init}	9.6×10^{-4}	2.1×10^{-3}
volume recombination coefficient, k_{vol} / pC^{-1}	2.1×10^{-3}	1.8×10^{-3}

Radial non-uniformity correction

At the NPL, no correction was applied to account for the non-uniformity of the beam across the transfer chambers. The correction factors for the radial non-uniformity calculated by the BIPM from the measured beam profiles in water are summarized in Table 8. For consistency, no correction was applied and a relative standard uncertainty of 5 parts in 10^4 is included in Table 15.

Table 8. BIPM and NPL correction factors for the NPL transfer chambers[(1)]

Radiation quality		6 MV	10 MV	15 MV	18 MV
ion recombination $k_{s,tr\ ch}$ NE 2611A-203	Niatel	1.0043	1.0077	–	1.0093
	TRS 398	1.0043	1.0072	–	1.0093
	NPL[(2)]	1.0069	1.0096	1.0113	–
ion recombination $k_{s,tr\ ch}$ NPL 2611-1007	Niatel	1.0049	1.0078	–	1.0092
	TRS 398	1.0049	1.0072	–	1.0093
	NPL[(2)]	1.0069	1.0096	1.0112	–
radial non-uniformity $k_{rn,tr\ ch}$	BIPM	1.0000	0.9990	–	1.0000

[(1)] At the BIPM, the ion recombination correction factors were measured at 10 g cm^{-2} depth in water at 6, 10 and 18 MV. At the NPL, the ion recombination correction factors were measured at 5 g cm^{-2} depth in water at 6 and 10 MV and at 7 g cm^{-2} depth in water at 15 MV, hence the difference between the numerical values of the correction factors at the BIPM (based on Niatel and TRS 398) and at the NPL.

[(2)] Using the method described by Burns and Rosser (1990)

Variation of $N_{D\mathrm{w}}$ with depth in water

NPL calibrations were carried out at 5 g cm^{-2} depth in water (6 and 10 MV) and 7 g cm^{-2} depth in water (15 MV), whereas all BIPM measurements were carried out at 10 g cm^{-2} depth in water (6, 10 and 18 MV). To account for any possible effect on the NPL calibration coefficients $N_{D\mathrm{w}}$ when using the transfer chambers at 10 g cm^{-2} depth in water, the changes with depth of the gradient of the tissue-maximum ratio (TMR) and of the stopping power ratio (SPR), water to air, were considered.

Tissue-maximum ratio (TMR) effect:

When using the NPL calibrated transfer chambers at a depth of 10 g cm^{-2} in water, the change of the gradient of TMR between the NPL reference depth (5 or 7 g cm^{-2}) and the BIPM reference depth (10 g cm^{-2}) was considered over the distance between the reference point and the effective point of measurement (EPOM). For megavoltage photon beams measured with cylindrical ionisation chambers, the EPOM is shifted from the reference point at the centre of the chamber towards the radiation source by a distance equal to 0.6 × r (IAEA 2000, IAEA 2024). With an approximate inner radius of the air cavity of NE 2611A and NPL 2611 thimble chambers of r = 0.4 cm, the difference between the reference point and the EPOM of the chamber is 0.6 × 0.4 cm = 0.24 cm. However, Tessier and Kawrakow (2010) concluded that an upstream EPOM shift of 0.6 × r is an overestimate by up to 25% for reference class thimble ion chambers in high energy photon beams. Although this study did not include type 2611 thimble chambers, the chamber dimensions are similar to those of some of the chambers listed therein. Using a revised EPOM shift of 0.45 × 0.4 cm = 0.18 cm, the mean TMR differences between the NPL reference depths and 10 g cm^{-2} for all beam qualities used for this comparison, i.e. 6, 10, 15 and 18 MV were found to be -0.08%, based on the TMRs listed in BJR (1996).

This evaluation of the change of $N_{D\mathrm{w}}$ is based on an estimated TMR gradient change and an estimated EPOM shift. Therefore, we do not consider the 0.08% change a definitive correction but an additional uncertainty component.

Stopping power ratio (SPR) effect:

The stopping power ratio water to air is the main contributing factor of the variation with beam quality in an ionisation chamber's absorbed dose to water calibration coefficient. Booth and

Rogers' Monte Carlo based study (Booth and Rogers 2010) included an investigation of the effect of the SPR as a function of depth in water. It concluded that for typical radiotherapy photon beam qualities ranging from ^{60}Co to 24 MV, the difference in stopping power ratio (SPR) between depths of 5 cm and 10 cm is less than 0.05% for all beams.

An additional uncertainty for the TMR and SPR effects on $N_{D\text{w}}$ at 5, 7 and 10 g cm^{-2} depth in water is included in Table 15. The combined relative standard uncertainty was calculated by adding 0.08% and 0.05% in quadrature, i.e. 0.09% (k = 1).

6. Results of the comparison

Measurements. The transfer chambers were set up and measured by the BIPM on two separate occasions. The results were reproducible to better than 4 parts in 10^4. At the NPL, the chambers were calibrated on two separate occasions, once before the measurements at the BIPM and once after the return of the chambers. The reproducibility at the NPL is estimated to be 7 parts in 10^4. The mean value of the NPL calibration coefficients measured before and after the BIPM measurements for each transfer chamber and the BIPM results are presented in Table 9 and in Figure 3. A quadratic fit is also included in Figure 3.

Data analysis. As shown in Table 1, the MV beams available at each radiation facility are different, thus the $\text{TPR}_{20,10}$ values also differ. As the usual practice is to evaluate the comparison results for the BIPM $\text{TPR}_{20,10}$ values, the quadratic fit of the NPL results was used to calculate the extrapolated value for the $\text{TPR}_{20,10}$ corresponding to the BIPM 18 MV quality. A quadratic fit was also applied to the BIPM results to derive the calibration coefficient for the 15 MV beam quality. Both the interpolated and extrapolated values give consistent comparison results, demonstrating that the extrapolation procedure is appropriate for use in this comparison. The results calculated in this way are included in Table 9.

Results. The comparison result, $R_{D,\text{w,NPL}}$, is expressed in the form

$$R_{D,\text{w,NPL}} = N_{D,\text{w,NPL}} / N_{D,\text{w,BIPM}} \qquad (10)$$

where $N_{D,\text{w,NPL}}$ is the mean of the values measured before and after the measurements at the BIPM for each radiation beam.

Table 9. Calibration coefficients for the transfer chambers

Radiation quality $\text{TPR}_{20,10}$	NPL 6 MV 0.682	BIPM 6 MV 0.686	10 MV 0.733	NPL 15 MV 0.758	BIPM 18 MV 0.774
NE 2611A-203					
$N_{D,\text{w,NPL}}$ / Gy µC^{-1}	103.06	103.01[a]	102.16	101.49	100.99 [a]
$N_{D,\text{w,BIPM}}$ / Gy µC^{-1}	–	102.92	102.30	101.64 [b]	101.12
$N_{D,\text{w,NPL}}/N_{D,\text{w,BIPM}}$	–	1.0009	0.9986	0.9985	0.9987
NPL 2611-1007					
$N_{D,\text{w,NPL}}$ / Gy µC^{-1}	101.24	101.19[a]	100.35	99.69	99.21[a]
$N_{D,\text{w,BIPM}}$ / Gy µC^{-1}	–	101.09	100.53	99.90[b]	99.40
$N_{D,\text{w,NPL}}/N_{D,\text{w,BIPM}}$	–	1.0010	0.9982	0.9979	0.9981

[a] $N_{D,\text{w}}$ calculated for the BIPM 6 MV and 18 MV $\text{TPR}_{20,10}$ using the quadratic fit to the NPL results

[b] $N_{D,\text{w}}$ calculated for the NPL 15 MV $\text{TPR}_{20,10}$ using the quadratic fit to the BIPM results

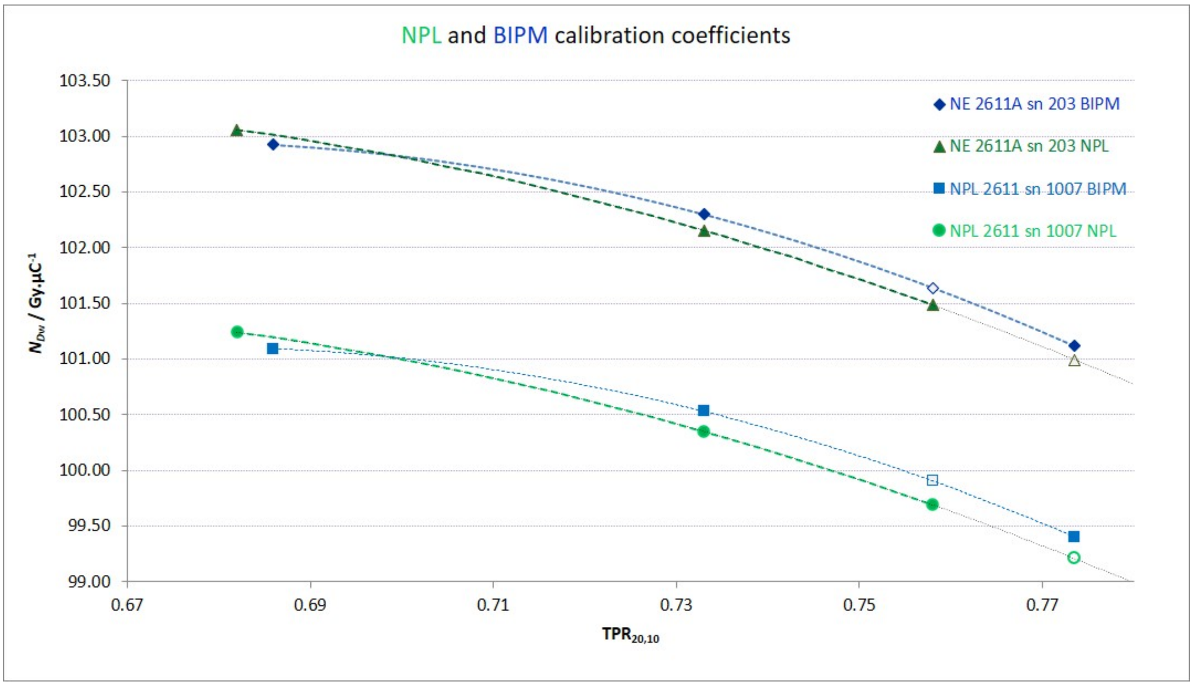

Figure 3. Calibration coefficients of the NE 2611A-203 and NPL 2611-1007 transfer chambers measured by each laboratory fitted using a quadratic function

The results $R_{D,\mathrm{w,NPL}}$ in Table 10 are evaluated as the mean for the two transfer chambers.

Table 10. **Comparison results**

Radiation quality	6 MV	10 MV	18 MV
$N_{D,\mathrm{w,NPL}}/N_{D,\mathrm{w,BIPM}}$ using NE 2611A-203	1.0009	0.9986	0.9987
$N_{D,\mathrm{w,NPL}}/N_{D,\mathrm{w,BIPM}}$ using NPL 2611-1007	1.0010	0.9982	0.9981
s_{tr}	0.0001	0.0002	0.0003
$R_{D,\mathrm{w,NPL}}$	1.0009	0.9984	0.9984

For each quality, the corresponding uncertainty s_{tr} is the standard uncertainty of the mean of the ratios $N_{D,\mathrm{w,NPL}}/N_{D,\mathrm{w,BIPM}}$, calculated for each transfer chamber. The mean value of s_{tr} for the three qualities, $s_{\mathrm{tr,comp}} = 0.0002$, is a global representation of the comparison uncertainty arising from the transfer chambers and is included in Table 15.

The values $N_{D,\mathrm{w,NPL}}$ measured before and after the measurements at the BIPM give rise to a relative standard deviation for each transfer chamber, whose root mean square value is taken as a representation of the stability of the transfer chambers. The stability is estimated to be 2 parts in 10^4 and is included in Table 15.

The results shown in Table 10 demonstrate the agreement between the two standards for absorbed dose to water within the relative standard uncertainty of the comparison of 7.7 parts in 10^3 evaluated below.

Uncertainties. The uncertainties associated with the BIPM primary standard and the calibration of the BIPM reference chamber are listed in Table 11.

Table 11. Uncertainties associated with the BIPM standard and the calibration of the BIPM reference chamber

Relative standard uncertainty [(1)]	100 $u_{i\mathrm{A}}$	100 $u_{i\mathrm{B}}$
$N_{D,\mathrm{c,st}}$	0.23	0.14
$C_{\mathrm{w,c}}$	0.05	0.25
$Q_{\mathrm{w,st}}/Q_{\mathrm{w,ref\ ch}}$	0.05	0.05
$k_{\mathrm{rn,st}}$	–	0.10
$k_{\mathrm{s,st}}$	–	0.05
$k_{\mathrm{vol,st}}$	–	0.03
depth standard	–	0.05
$k_{\mathrm{rn,ref\ ch}}$ [(2)]	–	0.03
$k_{\mathrm{s,ref\ ch}}$ [(2)]	–	0.03
depth BIPM reference chamber	–	0.05
stability $Q_{\mathrm{w,st}}/Q_{\mathrm{w,ref\ ch}}$	0.06	–
$N_{D,\mathrm{w,ref\ ch}}$	0.25	0.32

(1) Expressed as one standard deviation.
u_{iA} represents the relative uncertainty estimated by statistical methods, type A
u_{iB} represents the relative uncertainty estimated by other methods, type B

(2) Uncertainty removed from the analysis when the reference chamber is used to calibrate the transfer chamber

Table 12 summarizes the BIPM uncertainties associated with the calibration of the NPL transfer chambers used for the comparison.

Table 12. Uncertainties associated with the calibration of the NPL transfer chambers by the BIPM

Relative standard uncertainty	100 $u_{i\mathrm{A}}$	100 $u_{i\mathrm{B}}$
$N_{D,\mathrm{w,ref\ ch}}$	0.25	0.32
$Q_{\mathrm{w,ref\ ch}}/Q_{\mathrm{w,tr\ ch}}$	0.04	0.05
depth of the BIPM reference chamber	–	0.05
depth of the transfer chamber	–	0.05
$k_{\mathrm{s,tr\ ch}}$	–	0.03
short-term reproducibility	0.04	–
$N_{D,\mathrm{w,BIPM}}$	0.25	0.33

The uncertainties associated with the NPL primary standard and the calibration of the reference standard chambers are listed in Table 13. Table 14 summarizes the NPL uncertainties associated with the calibration of the NPL transfer chambers used for the comparison. The combined standard uncertainty u_{c} for the comparison results $R_{D,\mathrm{w,NPL}}$ is presented in Table 15.

Table 13. Uncertainties associated with the NPL standard

Relative standard uncertainty		100 u_{iA}	100 u_{iB}
Calorimetry			
$m_{core,eff}$	effective mass of the core / g	<0.01	0.01
$k_{z,cal}$	inverse square correction for source-to-core distance	–	0.10
$k_{d,cal}$	reference depth in graphite	<0.01	<0.01
$k_{rn,cal}$	radial beam non-uniformity correction for the calorimeter	–	0.03
$k_{an,cal}$	axial beam non-uniformity correction for the calorimeter	–	0.01
	core alignment on beam axis	–	<0.01
Monte Carlo considerations			
$k_{gap} \times k_{imp} \times k_{geom}$	product of MC calculated factors (1)	0.10	0.10
	source and calorimeter geometry modelling	–	0.10
	MC self-consistency, transport parameters	–	0.10
Electrical calibrations			
	electronics and thermistor calibrations	0.20	0.08
Heat capacity			
c_p	specific heat capacity of core graphite sample (2) / J kg^{-1} K^{-1}	0.28	0.08
k_c	specific heat capacity correction factor (3)	–	0.10
Calorimeter measurements			
	calorimeter data analysis	–	0.16
	repeatability of calorimetry results	0.10	–
Ionometry - Reference chamber measurements in graphite			
k_{elec}	electrometer calibration	–	0.10
$k_{elec,res}$	electrometer resolution	–	0.03
k_{ion}	ion recombination	–	0.03
$k_{z,cham}$	inverse square correction for source-to-chamber distance	–	0.10
$k_{rn,cham}$	radial beam non-uniformity correction for the ion chamber	–	0.01
T	air temperature / K	–	0.06
p	air pressure / kPa	–	0.05
RH	relative humidity	–	0.10
	ion chamber repeatability	0.03	–
Graphite to water conversion			
N_w / N_g	conversion of absorbed dose from graphite to water (4)	0.25	0.23
$N_{D,w,\text{ NPL ref cham}}$		0.45	0.42

(1) Monte Carlo calculated correction factors for the effects of the vacuum gaps in the calorimeter, the non-graphite impurities in the core and the difference between the geometries of the calorimeter and the graphite phantom for the reference chamber measurements, including differences in the water-equivalent depths of the reference points

(2) The specific heat capacity of a sample of graphite manufactured from the same batch as the calorimeter core at T = 25 °C.

(3) The correction factor applied to take into account the effect on the temperature rise of the graphite due to the differing values of heat capacity of the non-graphite components within the core, i.e. the thermistors and epoxy glue

(4) The type A and B uncertainties are those shown in Pearce *et al.* (2011), which are currently reported by the NPL for the ^{60}Co beam quality as well as all clinical linac MV photon beam qualities for absorbed dose to water calibrations

Table 14. Uncertainties associated with the calibration of the transfer chambers at the NPL

Relative standard uncertainty		100 $u_{i\mathrm{A}}$	100 $u_{i\mathrm{B}}$
Reference chamber calibration coefficient in terms of D_w			
$N_{\mathrm{Dw,\ NPL\ ref\ cham}}$	reference chamber calibration coefficient	0.45	0.42
Reference chamber and transfer chamber measurements in water			
$k_{\mathrm{elec,ref\_cham}}$	electrometer calibration	–	0.10
$k_{\mathrm{elec,ref\_cham,res}}$	electrometer resolution	–	0.03
$k_{\mathrm{ion,ref\_cham}}$	ion recombination	–	0.03
$T_{\mathrm{ref\_cham}}$	air temperature / K	–	0.06
$p_{\mathrm{ref\_cham}}$	air pressure / kPa	–	0.05
$R_{\mathrm{ref\_cham}}$	reference ion chamber repeatability	0.05	–
$R_{\mathrm{trans\_cham}}$	transfer ion chamber repeatability	0.07	–
$N_{D,\mathrm{w,\ NPL\ trans\ cham}}$		0.46	0.44

Table 15. Uncertainties associated with the comparison result

Relative standard uncertainty	100 $u_{i\mathrm{A}}$	100 $u_{i\mathrm{B}}$
$N_{D,\mathrm{w,NPL}}/N_{D,\mathrm{w,BIPM}}$	0.52	0.55
variation of N_{Dw} with depth in water	–	0.09
interpolation procedure	–	0.02
radial non-uniformity	–	0.05
transfer chambers $s_{\mathrm{tr,comp}}$	0.02	–
stability of transfer chambers	0.02	–
combined standard uncertainty $R_{D,\mathrm{w,NPL}}$	0.77	

7. Degrees of equivalence

Following a decision of the CCRI, the BIPM determination of the dosimetric quantity, here $D_{\mathrm{w,BIPM}}$, is taken as the key comparison reference value (KCRV) (Allisy *et al.* 2009). It follows that for each NMI, i, having a BIPM comparison result x_i with combined standard uncertainty u_i, the degree of equivalence with respect to the reference value is the relative difference $D_i = (D_{\mathrm{w}i} - D_{\mathrm{w,BIPM}i}) / D_{\mathrm{w,BIPM}i} = x_i - 1$ and its expanded uncertainty $U_i = 2\,u_i$.

Table 16 gives the values for D_i and U_i for each NMI, i, taken from the BIPM key comparison database (KCDB 2026) and this report. These data are presented graphically in Figure 4.

Note that these data, while correct at the time of publication of the present report, become out of date as laboratories make new comparisons. In accordance with the validity rules for comparison data agreed by the CCRI(I), results older than 15 years are considered no longer valid and have been removed from the KCDB. The formal results under the CIPM MRA are those available in the key comparison database (KCDB 2026).

Table 16. **Degrees of equivalence**

Beam quality corresponding to measured $TPR_{20,10}$ between 0.63 (included) and 0.71 (excluded)

Lab *i*	D_i / (mGy / Gy)	U_i
NIST	3.5	11.4
VSL	-4.1	10.8
NMIJ	-3.4	9.4
NIM	-8.3	12.0
KRISS	7.8	12.0
METAS	-1.7	13.2
LNE-LNHB	-2.3	11.8
NRC	4.0	11.6
PTB	2.6	11.4
ARPANSA	-4.5	12.4
GUM	4.0	12.8
NPL	0.9	15.4

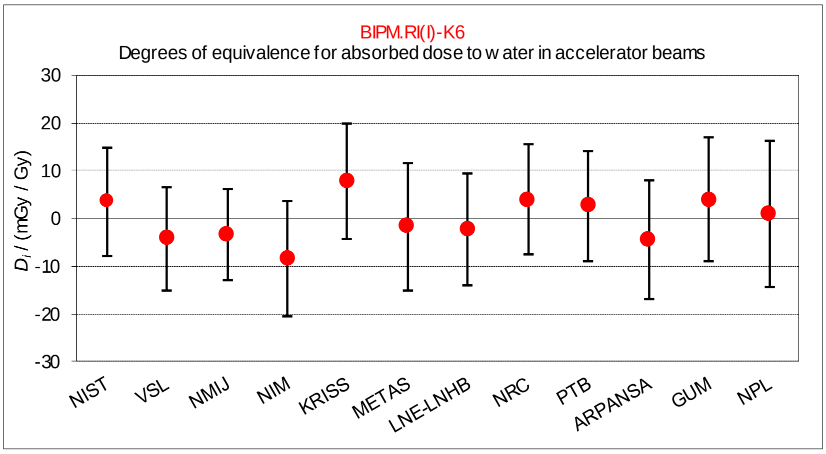

Figure 4a. Graph of the degrees of equivalence with the KCRV

Beam quality corresponding to measured $TPR_{20,10}$ between 0.71 (included) and 0.77 (excluded)

Lab *i*	D_i / (mGy / Gy)	U_i
VSL	-4.2	12.8
NMIJ	-4.1	11.0
NIM	-5.9	11.8
KRISS	5.6	12.0
METAS	-3.2	13.2
LNE-LNHB	-3.8	11.8
NRC	3	11.6
PTB	-0.6	11.4
ARPANSA	-5.1	12.4
GUM	3.7	12.8
NPL	-1.6	15.4

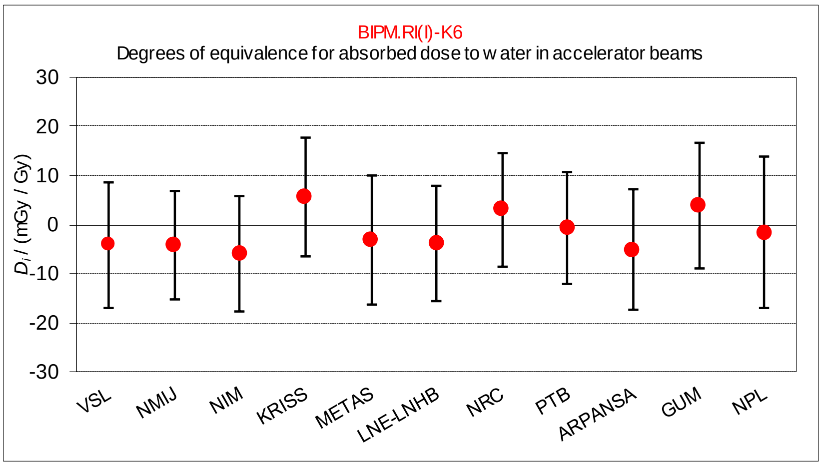

Figure 4b. Graph of the degrees of equivalence with the KCRV

Beam quality corresponding to measured $TPR_{20,10}$ between 0.77 (included) and 0.81(included)

Lab *i*	D_i / (mGy / Gy)	U_i
NIST	-4.2	11.8
VSL	1.0	14.8
KRISS	8.5	12.0
METAS	-1.2	13.2
LNE-LNHB	-4.4	11.8
NRC	3.9	11.6
PTB	-0.3	11.4
ARPANSA	-4.9	12.4
NPL	-1.6	15.4

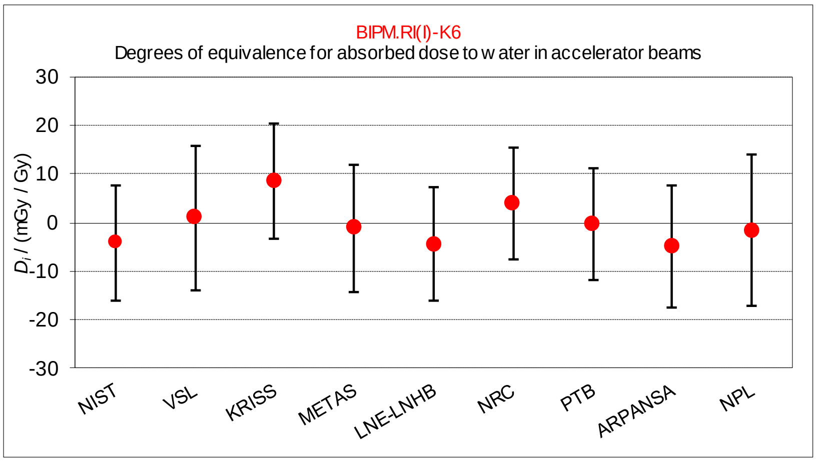

Figure 4c. Graph of the degrees of equivalence with the KCRV

8. Conclusions

A new key comparison has been carried out between the NPL and the BIPM standards for absorbed dose to water in accelerator photon beams, using two ionization chambers as transfer chambers. The comparison result is evaluated as the ratio of the calibration coefficients measured by the NPL and the BIPM. The results show the standards to be in agreement within the standard uncertainty of the comparison of 7.7 parts in 10^3. The present results are in agreement with the results of the previous comparison within the uncertainties: 0.9973(62) at 6 MV, 0.9995(66) at 10 MV and 0.9957(81) at 25 MV (Picard et al. 2015). The measurements were carried out in the Elekta Synergy linear accelerator at the NPL in 2013.

When compared with the results for the other laboratories that have carried out comparisons in terms of absorbed dose to water, the NPL standard for absorbed dose to water is in good agreement with the ensemble of results.

References

Allisy P J, Burns D T and Andreo P 2009 International framework of traceability for radiation dosimetry quantities *Metrologia* **46(2)** S1-S8 (DOI 10.1088/0026-1394/46/2/S01)

BJR 1996 Central Axis Depth Dose Data for Use in Radiotherapy:1996 *British Journal of Radiology* BJR Supplement 25

Booth A and Rogers D W O 1995 Monte Carlo Study of Effects of Phantom Size, Radial Position, and Depth on Photon Beam Calibration *NRC report* PIRS-507

Boutillon M 1998 Volume recombination parameter in ionization chambers *Phys. Med. Biol.* **43** 2061-2072 (DOI 10.1088/0031-9155/**43**/8/005)

Burns J E and Rosser K E 1990 Saturation correction for the NE 2560/1 dosemeter in photon dosimetry *Phys. Med. Biol.* **35** 687-693 (DOI 10.1088/0031-9155/35/5/009)

International Atomic Energy Agency 2024 Absorbed Dose Determination in External Beam Radiotherapy. An International Code of Practice for Dosimetry Based in Standards of Absorbed Dose to Water *Technical Report Series* No 398 (Rev. 1) (IAEA Vienna)

International Atomic Energy Agency 2000 Absorbed Dose Determination in External Beam Radiotherapy. An International Code of Practice for Dosimetry Based in Standards of Absorbed Dose to Water *Technical Report Series* No 398 (IAEA Vienna)

KCDB 2026 BIPM Key Comparison Database Measurement of absorbed dose to water for high-energy photon beams BIPM.RI(I)-K6

Kessler C and Burns D T 2024 Measurement conditions and uncertainties for the comparison and calibration of national dosimetric standards at the BIPM *Rapport BIPM*-2024/04 (DOI 10.59161/Rapport202404)

Kessler C, Burns D T, Kelly M, Maughan D J, Bass G A, Shipley D R, Sander T, Lee N D, Cashmore M and Duane S 2019a Comparison of the standards for absorbed dose to water of the NPL, United Kingdom and the BIPM for ^{60}Co γ rays *Metrologia* **56**(1A) 06008 (DOI 10.1088/0026-1394/56/1A/06008)

Kessler C, Burns D T, Roger P, Kottler C, Vörös S and Peier P 2019b Comparison BIPM.RI(I)-K6 of the standards for absorbed dose to water of the METAS, Switzerland and the BIPM in accelerator photon beams *Metrologia* **56** *Tech. Suppl.* 06001 (DOI 10.1088/0026-1394/56/1A/06001)

Nutbrown R F, Duane S, Shipley D R and Thomas R A S 2002 Evaluation of factors to convert absorbed dose calibrations from graphite to water for the NPL high-energy photon calibration service *Phys. Med. Biol*. **47** 441-454 (DOI 10.1088/0031-9155/47/3/306)

Pearce J A D, Shipley D R and Duane S 2011 Transfer of the UK absorbed dose primary standard for photon beams from the research linac to the clinical linac at NPL *Metrologia* **48** 365-374 (DOI 10.1088/0026-1394/48/5/018)

Pearce J A D, Shipley D R and Duane S 2010 Re-establishing the absorbed dose primary standard for photon beams on the NPL clinical linac *NPL report* IR 24

Picard S, Burns D T and Roger P 2009 Construction of an Absorbed-Dose Graphite Calorimeter *Rapport* BIPM-2009/01 (https://www.bipm.org/fr/publications/rapports-bipm-2001-2010)

Picard S, Burns D T and Ostrowsky A 2011 Determination of the recombination correction for the BIPM parallel-plate ionization chamber type in a pulsed photon beam *Rapport* BIPM-2011/06 (https://www.bipm.org/fr/publications/rapports-bipm)

Picard S, Burns D T, Roger P, Duane S, Bass G A, Manning J W and Shipley D R 2015 Key comparison BIPM.RI(I)-K6 of the standards for absorbed dose to water at 5 g cm^{-2} and 7 g cm^{-2} of the NPL, United Kingdom and the BIPM in accelerator photon beams *Metrologia* **52** *Tech. Suppl.* 06010 (DOI 10.1088/0026-1394/52/1A/06010)

Sander T, Bass G A, Cashmore M T D, Duane S, Galer S E, Homer M J, Lee N D, Nutbrown R F and Shipley D R 2017 The NPL absorbed dose primary standard graphite calorimeter (2015 design) for ^{60}Co: summary of correction and conversion factors *NPL report* IR 45

Seuntjens J and Duane S 2009 Photon absorbed dose standards *Metrologia* **46** S39-S58 (DOI 10.1088/0026-1394/46/2/S04)

Tessier F and Kawrakow I 2010 Effective point of measurement of thimble ion chambers in megavoltage photon beams *Med. Phys.* **37**(1) 96-107 (DOI 10.1118/1.3266750)